15th Triennial World Congress, Barcelona, Spain

THE ANALYSIS AND CONTROL OF THE ALSTOM GASIFIER BENCHMARK PROBLEM

C S Chin and N Munro

Control Systems Centre,
Department of Electrical Engineering and Electronics,
University of Manchester Institute of Science and Technology,
Manchester, UK.

Abstract: This paper considers the analysis and controller design for the ALSTOM gasifier system. The inherent properties of this highly coupled multivariable system are studied. Minimal realizations of the system models at the three operating points to be considered are determined, and the numerical condition of the system is improved. Model order reduction methods are applied to simplify the subsequent design. A controller is designed using the LQG/LTR technique at the 100% load condition, and the robustness of this controller at other load conditions is assessed. No violation in the desired performance specifications was encountered. *Copyright © 2002 IFAC.*

Keywords: Conditioning, structure, order reduction, controller design, sensitivity.

1. INTRODUCTION

The purpose of this paper is to describe a case study carried out on the ALSTOM benchmark challenge on gasifier control. Although several papers have already been published on the control of this gasifier system, the poor nature of the numerical data describing the linear models of this system has limited some of the results previously obtained.

A detailed description of the gasifier, which generates gas used to power gas turbines driving electrical generators, along with several design studies, is available (Dixon, *et al.*, 2000). However, here, only a brief description of the gasifier is given, along with the desired performance specifications. This is followed by various tests to determine the inherent properties of this system. Minimal realizations of the system models to be considered are created. Osborne's pre-conditioning is applied to the state-space model matrices to improve the numerical conditioning. Control system design using the Linear Quadratic Gaussian approach with Loop Transfer Recovery (LQG/LTR) is then carried out on the gasifier system. Lastly, sets of criteria used to compare this design with controllers designed for the gasifier system using other methods (Chin, 2001) are also discussed.

2. GASIFIER SYSTEM DESCRIPTION

A schematic diagram of the gasifier is shown in Fig 1. It is a nonlinear multivariable system, having four outputs to be controlled with a high degree of cross coupling between them. The control inputs are ordered as the char extraction flow in kg/s (WCHR), air mass flow in kg/s (WAIR), coal flow rate in kg/s (WCOL), steam mass flow in kg/s (WSTM), and also a disturbance input in N/m^2 (PSINK). The outputs to be controlled are ordered as fuel gas calorific value in J/kg (CVGAS), bed mass in kg (MASS), fuel gas pressure in N/m^2 (PGAS) and fuel gas temperature in K (TGAS). By initially neglecting the effects of the input disturbances, PSINK, and noting that limestone mass flow in kg/s (WLS) absorbs sulphur in the coal WCOL with a fixed ratio of 1:10, this leaves effectively four inputs for control design. Hence, the gasifier becomes a 4×4 square system.

The gasifier is described by 3 state-space models of 25^{th} order obtained from a nonlinear model by linearisation about the 100%, 50% and 0% load conditions. In the following, $G_{100\%}$ will denote the plant model at the 100% load condition. For the three cases to be considered, the gasifier models used are in continuous linear time invariant state space form:

$$\begin{aligned} \dot{x}(t) &= Ax(t) + Bu(t) \\ y(t) &= Cx(t) + Du(t) \end{aligned} \tag{1}$$

The aim of this benchmark challenge is to design a controller at the 100% operating condition that satisfies the following performance specifications: -

1. The calorific value fluctuation should be minimized and always be within ±10 kJ/kg.
2. The pressure fluctuation should be minimized and always be within ±0.1 bar.
3. The bed mass should remain within ±500 kg from the set point.
4. The temperature fluctuation should be kept to a minimum and always be within ±1 deg C.
5. The input flow limits and the input rate of change limits, shown in Table 1, cannot be exceeded when a step or sine wave pressure disturbance are applied.

Table 1. Control input limits.

Input	Maximim (kg/s)	Rate (kg/s^2)
Coal inlet flow	10	0.1
Air inlet flow	20	1.0
Steam inlet flow	6.0	1.0
Char extraction	3.5	0.2

In addition, the robustness of the controller determined at the 100% load condition is to be evaluated at the 50% and 0% load conditions, when a pressure step disturbance (PSINK) of 0.2 bar and a sine wave pressure disturbance of amplitude 0.2 bar at a frequency of 0.04 Hz are applied to the system, at t = 30s, by running the system simulation for 300 seconds and calculating the Integral of Absolute Error (IAE) for the calorific value and pressure outputs over this time interval.

3. INHERENT PROPERTIES TESTS

Before starting on the development of a controller, several tests were performed using the state-space model at the 100% load condition.

Open-loop Stability. The open-loop 25^{th} order system is stable, with eigenvalues

$$\lambda_i = \{-33.125, -1.0056, -0.3956, -0.1317, -0.1084, -0.1055, -0.0301, -0.0070, -0.0568, -0.0568, -0.0568, -0.0568, -0.0568, -0.0568, -0.0568, -0.0568, -0.0568, -0.0568, -0.0002, -0.0003, -0.0007, -0.0004\pm0.0002i, -0.0007\pm0.0004i\}$$

as confirmed by the time responses in Figure 2.

Minimal Realizations. Using the MATLAB tests for controllability and observability gave extraneous results due to the poor condition number of the A matrix, which was found to be $5.2\text{x}10^{19}$ (using the infinity norm). However, it was found that the original A matrix is reducible to a block lower triangular form using row and column permutations, and yielded

$$\text{Ar} = \begin{bmatrix} A_{11} & 0 \\ A_{21} & A_{22} \end{bmatrix} \quad \text{Br} = \begin{bmatrix} 0 \\ B_{21} \end{bmatrix}$$
$$\text{Cr} = \begin{bmatrix} C_{11} & C_{12} \end{bmatrix} \quad \text{Dr} = \text{D} \tag{2}$$

where A_{11} and A_{22} are square matrices of dimensions 7 and 18, respectively, with A_{21} being a 18 x 7 matrix, and with A_{11} being diagonal. Since the corresponding block in the matrix B_r is also zero, the modes contained in A_{11}; namely, the eigenvalues λ = {-0.0568, -0.0568, -0.0568, -0.0568, -0.0568, -0.0568, -0.0002}; are uncontrollable. These can be removed by simply deleting rows and columns 1-7 of the matrix A_r, rows 1-7 of the matrix B_r, and columns 1-7 of the matrix C_r. This yields an 18^{th} order realization of the gasifier system, which turns out to be a minimal realization.

Pre-conditioning. Before performing any further numerical operations using the resulting state space minimal realization matrices, Osborne's numerical conditioning algorithm (1960) was applied to these matrices, and resulted in the condition number of the A-matrix being reduced from $5.1\text{x}10^{19}$ to $9.8\text{x}10^{6}$. This approach was compared with other norm-based scaling methods (Strang, 1976); namely, the one-norm, infinity-norm, and two-norm; and the results obtained are shown in Table 2, where the Sum of Absolute Error (SAE) between the original and resulting matrix elements is used.

Table 2: Comparison of various numerical pre-conditioning methods.

Norm Method	SAE	Maximum SAE
One-norm	$4.13\text{x}10^{-15}$	$10\text{x}10^{-16}$
Two-norm	$1.1\text{x}10^{-15}$	$5.5\text{x}10^{-16}$
Infinity-norm	$4.2\text{x}10^{-16}$	$1.5\text{x}10^{-16}$
Osborne	$2.7\text{x}10^{-8}$	$2.1\text{x}10^{-9}$

Interaction. The transfer function matrix of the scaled system was used to determine the interaction present in the gasifier system using Rosenbrock's row diagonal dominance Gershgorin discs, superimposed on the diagonal elements of the system frequency responses (Patel and Munro, 1982), as shown in Figure 3. These plots indicate that the system is highly interactive over all frequencies.

4. CONTROL STRUCTURE DESIGN

An important part of a multivariable design is the selection of the best input/output (I/O) pairing, which defines the control structure design problem (Jager, 2000).

The Relative Gain Array (Bristol, 1966) was determined for the 4 x 4 gasifier system $G_{100\%}$, as

$$\Lambda = \begin{bmatrix} 0.4133 & -0.0724 & 0.4187 & 0.2404 \\ \mathbf{0.5781} & -0.0302 & \mathbf{0.4246} & 0.0274 \\ 0.0150 & \mathbf{0.9066} & 0.0519 & 0.0265 \\ -0.0064 & 0.1959 & 0.1048 & \mathbf{0.7056} \end{bmatrix} \quad (3)$$

The coefficients of this matrix suggest that the first input (WCHR) should control the second output (MASS), since element (2,1) of Λ is the closest to 1 in this column. The remaining I/O pairs were determined similarly by examining the rest of the columns of Λ. And suggested that PGAS, CVGAS and TGAS are most suitably controlled by the WAIR, WCOL and WSTM, respectively. The system outputs were accordingly reordered using an appropriate row permutation matrix.

As the RGA in (3) was calculated at zero frequency, the RGA-number (Skogestad and Postlethwaite, 1995) was evaluated across the frequencies of interest for $G_{100\%}$ after the initial reordering of the outputs. The plots obtained showed that there is a slight decrease in the RGA number across all frequencies and this implies that the selected I/O pairs will have a beneficial effect on the diagonal dominance of the system. This I/O pairing was further confirmed by calculating the minimum of the Hankel singular values of the system, which were increased from 0.00379 to 0.256, after reordering the outputs.

5. PRELIMINARY DESIGN AND SCALING

As a desirable physical requirement, a PI controller; PI = k_p+k_i/s; that would tightly control the BED-MASS height directly using the char-offtake (WCHR) was designed, and resulted in a block diagonal dominant form of the resulting transfer function model G(s); i.e. the minimum singular value of the 1×1 and 3×3 diagonal blocks was greater than the maximum singular value of the off-diagonal blocks. This implies that this loop would be well decoupled from the remaining 3×3 subsystem. The closed-loop step response of the first loop was determined, and it was found that the rate of change of WCHR was well within the specified value of 0.2 kg/s^2.

The bandwidth of the resulting 3×3 subsystem of the gasifier, given by the minimum singular value of the loop gain L(jw), was found to be 0.005 rad/s. This is equivalent to a rise time of about 200 seconds, which is quite acceptable for this system, since it is a physically large system that requires a time of several hundred seconds to react.

The Perron-Frobenius design scaling approach (Mees, 1981), Edmunds' design scaling and I/O pairing method (Edmunds, 1998), and the one-norm scaling were tried, and it was found that the Edmunds' scaling applied at 0.008 r/s gave a more diagonal dominant system, as shown in Figure 4, and also produced the I/O pairings, WCOL-TGAS, WAIR-CVGAS and WSTM-PGAS, for the remaining 3x3 sub-system design. This led to the final control system structure shown in Figure 5.

6. MODEL ORDER REDUCTION

Since the remaining sub-system of the gasifier contains elements of 18th order, it was decided to determine a reduced order sub-system model, G_r. For comparison purposes, here only two methods are considered; namely, modal truncation method and the Schur balanced truncation method. Both time and frequency response tests were used to check for any significant deviation of the reduced order models obtained from the full-order model. The Hankel SVs for the Schur balanced truncation model, of order n_r = 8, were larger than those of the modal truncation model, which indicates that the former has better state controllability and observability properties than the latter.

7. DESIGN OF LQG/LTR CONTROLLER

The following steps are involved in determining a controller at the 100% load condition, using the Linear Quadratic Gaussian approach with Loop Transfer Recovery: -

1) Solve the Algebraic Riccati Equation (ARE); $$A^T P + PA + Q - PBR^{-1}B^T P = 0.$$
2) Determine the optimal state feedback gain; $$F = R^{-1}B^T P.$$
3) Solve the Filter Algebraic Riccati Equation; $$AP_e + P_e A^T + \Gamma W \Gamma^T - P_e C^T V^{-1} C P_e = 0.$$
4) Determine the optimal state estimator gain; $$F_e = PC^T V^{-1}.$$

The following are the weighting matrices used: -
$Q = C^T C$
Q_e = 0.005 x diag{0.5, 0.2 ,0.1 ,0.2, 0.3, 0.1, 0.3, 0.1, 0.9,0.1, 0.6, 0.8, 0.2, 0.7, 0.01, 0.02, 0.01, 0.1} + q^2BB^T
where q = 10, and

$$R = \begin{bmatrix} 35 & 0 & 0 \\ 0 & 25 & 0 \\ 0 & 0 & 21 \end{bmatrix} \qquad R_e = \begin{bmatrix} 0.5 & 0 & 0 \\ 0 & 0.4 & 0 \\ 0 & 0 & 0.1 \end{bmatrix} \quad (4)$$

By having a different weight in Q_e on each state, the corresponding output can be shaped. It was observed that the weights Q_{10}, Q_{12}, Q_{15}, Q_{17} and Q_{18} have a fairly high influence on the output MASS, while the Q_7, Q_9, Q_{10}, Q_{12}, Q_{15} and Q_{17} have a substantial effect on TGAS. The weights Q_1, Q_2, Q_5, Q_6, Q_{11}, Q_{13}, Q_{14} and Q_{16} seem to have no influence on any outputs.

The required performance tests for the LQG/LTR controller design were carried out for the specified step and sinusoidal disturbance inputs using SIMULINK. The results, for the step disturbance case are summarized in Table 3, and were obtained by only offsetting the steady state values provided from the inputs. The graphical results are presented here only for the 100% load conditions (Figure 6) for the specified simulation run time t = 300 seconds. The remaining parts of these time responses reach their steady-state values in a well behaved manner.

With the LQG/LTR controller design, all the input and output constraints are met at all load conditions. The input rates observed at all load conditions are very small and hence keep the outputs within the specified limits. The Integral of the Absolute value of the Error (IAE) associated with the CVGAS increases as the load condition decreases from 100% to 0%. This is not an unexpected trend, since the primary design was undertaken for the 100% load condition. On the other hand, with PGAS this does not seem to be the case, and this reduces progressively from the 100% load condition, through the 50% load condition, to the 0% load condition.

8. COMPARISON OF CONTROLLERS

Various criteria such as the output and input sensitivity (S), the robust stability (RS), the MIMO system asymptotic stability (MIMIO AS), the integral of error squared (ISE), internal stability, the order of the resulting controller (CO), and the condition number (CN) of the closed-loop system, were used to make a comparison with other designs carried out using LQR, LQG, H_2 optimizat, and H_∞ (Chin, 2001), but these designs are not presented here.

Table 4 gives a summary of the comparisons made using the criteria mentioned above, where a dash indicates criteria that are satisfied over the frequency range, and the sub-headings O and I refer to output and input, respectively. From this Table, it can be seen that the H_∞ optimization approach gives the highest order controller which exceeds that of the 18^{th} order minimal realisation of the gasifier plant itself. Also, when compared to its counterpart determined using H_2 optimization, or any other controller design method, the computational burden appears to be excessive.

For the LQG and LQG/LTR design, robust stability at the gasifier input, within the bandwidth of interest (ω_B = 0.005 r/s) could be met. Therefore, these designs are robustly stable for both plant output and input disturbances, when operating at the 50% and 0% load conditions. All controllers designed seem to satisfy the internal stability criteria. Hence, any signal injected at any point in the closed-loop system of the gasifier would result in a stable or bounded output at any other point.

The input and output sensitivity are met for all controller designs. This shows that the feedback system designed using any of the controllers is insenstive to a disturbance input, such as a step or sinusoidal function.

With these comments, the controllers considered are ranked as, LQG/LTR and LQG, followed by H_∞, then LQR and H_2. Note that this ranking is only with respect to the gasifier system being studied.

As observed, the LQR design is ranked quite low due to the violation of the robustness test. On the other hand, the H_2 design which uses a more natural norm should be able to fair better than the H_∞ design. However, it is ranked the last due its inability to meet some of the constraints in the performance specifications, as well as the higher order resulting closed-loop system and controller obtained from its formulation. In addition, the high condition number obtained from this design is taken into account. The H_∞ design is ranked after the LQG and LQG/LTR due to its high order controller. Merits such as the ability to produce a stabilized controller and a good measure on the robustness aspects are taken into account. The H_∞ controller complexity is deemed to be less attractive as compared with its robust competitor the LQG/LTR, which is simpler to implement in practice and gives moderately good robutness margins.

9. CONCLUSIONS

An LQG/LTR controller was designed at the 100% load condition, that satisfied the given performance specifications. Performance tests using this controller were carried out at the 50% and 0% load conditions with good results. Various other controllers designed at the 100% load condition were compared using various criteria. It was found the LQG/LTR, the LQG, and the H_∞ seemed to perform better than the other designs considered.

REFERENCES

Bristol, E.H. (1966). On a New Measure of Interactions for Multivariable Process Control, *IEEE Trans. Auto. Contr.*, **Vol. AC-11**, p 133-134.

Chin, C.S. (2001). *The Analysis and Model Order Reduction and Control of a Gasifier*, MSc. Dissertation, UMIST, Manchester.

Dixon, R.,, A.W. Pike and M. S. Donne (2000). The ALSTOM Benchmark Challenge on Gasifier Control, *Proc. Instn. Mech. Engrs, Part I, Journal of Systems and Control Engineering*, **Vol. 214 (16),** p 389-394.

Doyle, J.C. and G. Stein (1981). Multivariable Feedback Design: Concepts for a Classical Modern Synthesis, *IEEE Trans Auto. Contr.*,**Vol. AC-26 (1),** p 4-16.

Edmunds, J.M. (1998). Input and output scaling and reordering for diagonal dominance and block diagonal dominance, *Proc. IEE, Part D*, **145**, 523-530.

Jager, M.B. (2000). A Review of Methods for Input/Output Selection, *Automatica* **37**, p 487-510.

Mees, A.I. (1981). Achieving Diagonal Dominance, *System and Control Letters*, **Vol. 1 (3)**.

Osborne, E.E. (1960). On Preconditioning of Matrices, *J. of Assoc. of Computing Machinery*, **Vol. 7**, p 338-345.

Patel, E.V. and N. Munro (1982). *Multivariable System Theory and Design*, Pergamon Press, Oxford.

Postlethwaite, I., J.M. Edmunds and A.G.J. MacFarlane (1981). Principal Gains and Principal Phases in the Analysis of Linear Multivariable Feedback Systems, *IEEE Trans. Auto. Contr.*, **Vol. AC-26 (1),** p. 32-46.

Skogestad, S. and I. Postlethwaite (1995). *Multivariable Feedback Control Analysis and Design*, John Wiley.

Strang, G. (1976). *Linear Algebra and its Applications*, Academic Press.

Table 3: Results for the step disturbance at the 100 % load condition (left) and the 0% load condition (right)

	Minimum value	Maximum value	Peak value	IAE
WCHR	0.75	1.16	0.002	-
WCOL	8.43	9.68	0.013	-
WAIR	17.29	18.35	0.011	-
WSTM	2.60	2.87	0.004	-
MASS	10000.00	10002.07	-	-
TGAS	1205.66	1223.20	-	-
CVGAS	4356.91	4360.01	-	92.19
PGAS	1999.18	2000.38	-	30.37

	Minimum value	Maximum value	Peak value	IAE
WCHR	0.51	0.759	0.00079	-
WCOL	8.43	8.74	0.0119	-
WAIR	17.29	17.56	0.01036	-
WSTM	2.49	2.70	0.0041	-
MASS	10000.00	10000.12	-	-
TGAS	1222.16	1223.21	-	-
CVGAS	4359.84	4360.02	-	32.64
PGAS	1999.62	2000.42	-	82.46

Table 4: Summary of the criteria used for each controller design

	S		**RS**		**MIMO**	**ISE**	**CO**	**CN**	**RHP**
	O	**I**	**O**	**I**	**AS**				**ZEROS**
LQR	1	-	1	10	1	5×10^{7}	19	1.5×10^{8}	2
LQG	0.01	-	0.008	1×10^{-4}	0.01	1×10^{5}	19	1×10^{9}	1
LQR/LQG	0.01	-	0.008	1×10^{-4}	0.01	9×10^{4}	19	3×10^{9}	2
H_∞	-	-	0.01	0.01	-	4×10^{3}	19	3×10^{9}	4
H_2	-	-	0.01	0.01	-	2×10^{6}	19	4×10^{17}	8

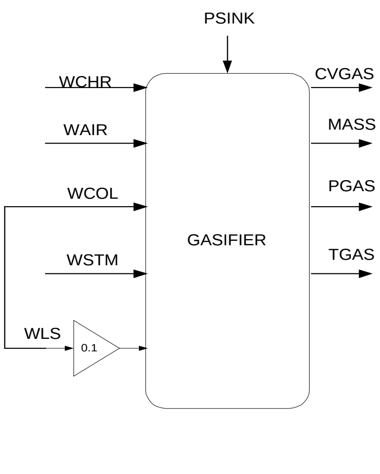

Figure 1: Schematic diagram of the gasifier

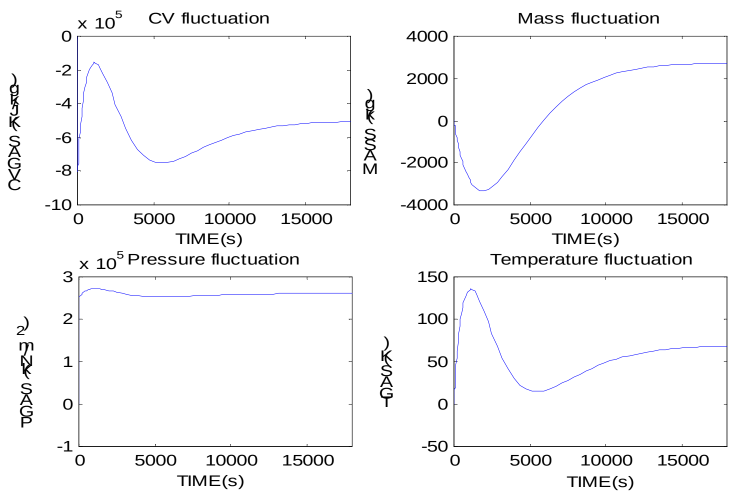

Figure 2: Open loop steady state responses

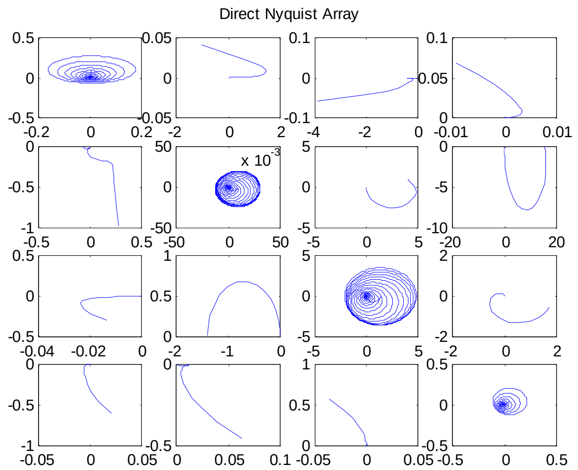

Figure 3: Direct Nyquist Array of the 4 x 4 gasifier

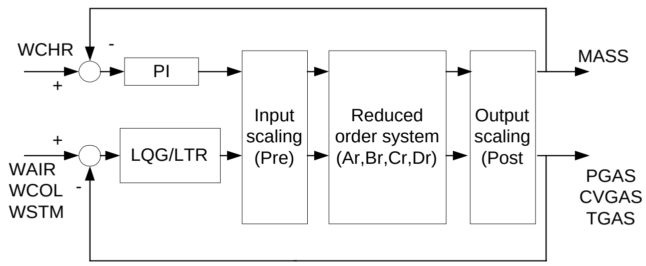

Figure 5: Final control structure

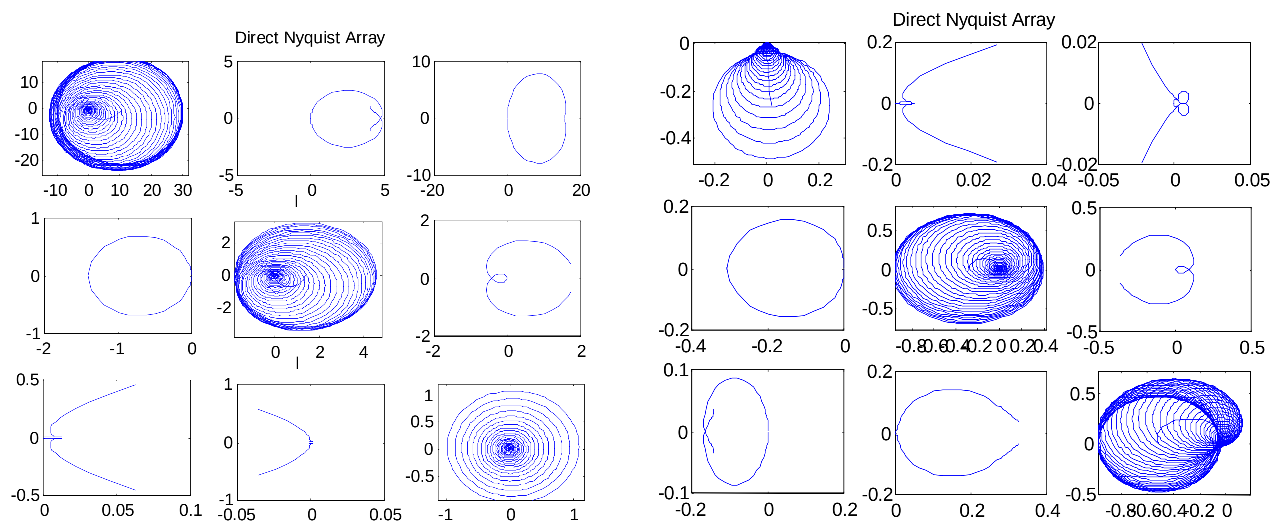

Figure 4: DNA of the system before and after scaling

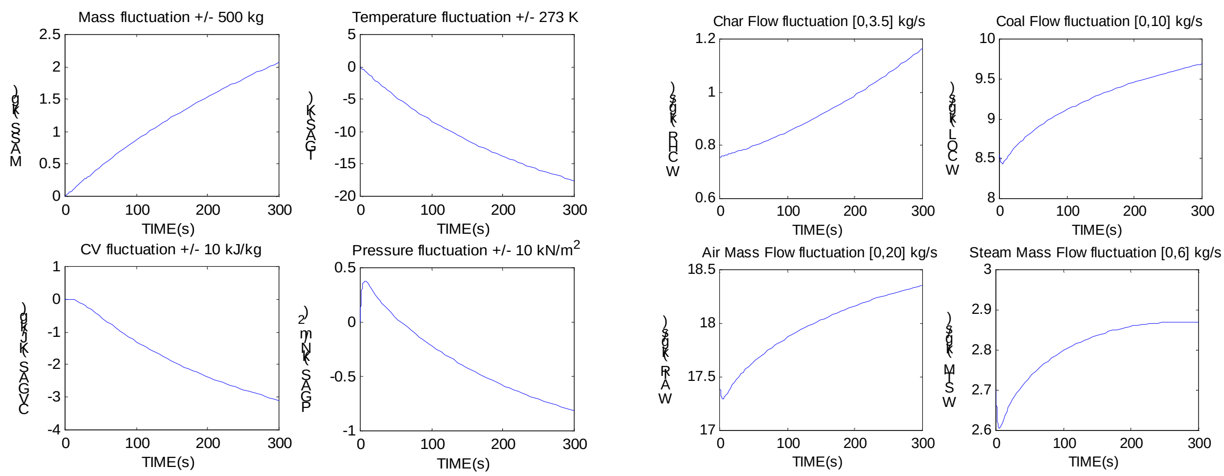

Figure 6: Gasifier outputs and inputs for a step pressure disturbance (100 % load condition)